1400

Commission of the European Communities

Sixth E.C.

Photovoltaic Solar Energy Conference

Proceedings of the International Conference, held in London, U.K., 15-19 April 1985

Edited by

W. PALZ
Commission of the European Communities, Brussels

and

F.C. TREBLE
C.E.C. Consultant, Farnborough, Hants., United Kingdom

D. REIDEL PUBLISHING COMPANY
A MEMBER OF THE KLUWER ACADEMIC PUBLISHERS GROUP
DORDRECHT / BOSTON / LANCASTER

THE USE OF A PULSED LASER FOR SHALLOW-JUNCTION PROCESSING

W. SINKE, A. POLMAN, W.G.J.H.M. VAN SARK and F.W. SARIS

FOM-Institute for Atomic and Molecular Physics,
Kruislaan 407, 1098 SJ Amsterdam, The Netherlands

Summary

Silicon solar cells have been prepared with a shallow junction, using low-energy (10 keV P^+) ion implantation and pulsed-laser annealing. Whereas the short-circuit current shows a maximum for the smallest emitter thickness ($\approx$ 0.1 μm) that can be obtained, it requires a thickness of $\approx$ 0.2 μm to optimize the open-circuit voltage. By using a new curve-fitting procedure, model parameters have been determined in a two-diodes description of the electrical characteristics of the cells. From these results, it is concluded that implantation-tail defects within the junction depletion region adversely affect the open-circuit voltage for very thin emitters.

1. INTRODUCTION

Recently, ion implantation in combination with pulsed-laser annealing (p.l.a.) has received considerable attention as a method to apply a p-n junction in crystalline silicon solar cells (1,2,3,4,5). The main reasons for this are the following:

[A] Using ion implantation, accurate dose control can be obtained.
[B] Bulk-material quality is not affected during processing because only low temperatures are involved.
[C] High-current ("hot") ion implantation, which is used to obtain a high throughput, results in partial recrystallization of the implanted layer. In such cases, solid-phase epitaxial regrowth by thermal annealing is unsuitable and liquid-phase regrowth (for instance p.l.a.) must be used.
[D] Using pulsed-laser annealing, one is not restricted to a Gaussian-like dopant profile and to the maximum solid solubility of the dopant, as is the case with classical diffusion. Thus, it becomes possible to realize a very shallow junction with a reasonable sheet resistance.
[E] Directed-beam processing like ion implantation and pulsed-laser annealing can be automated and controlled easily.

From the above arguments it is clear that ion implantation and pulsed-laser annealing form a suitable technique for the processing of low-grade starting material (e.g. polycrystalline solar-grade silicon): the minority-carrier diffusion length in the bulk and hence, the long-wavelength response of the cell will not be affected during processing. In addition, the short-wavelength response can be improved by applying a very shallow emitter. Therefore, it should be possible to obtain a reasonable short-circuit current even in this kind of material.

However, in most studies of p.l.a. for junction processing no special attention is paid to the influence of emitter thickness on the short-circuit current. Therefore, it is not clear what is to be gained by reducing the junction depth. In addition, for n-type implants like phosphorus, a

relatively low open-circuit voltage is sometimes obtained (4). The origin of this effect is still not clear.

In this paper we present the results of a study of the relation between laser energy density, emitter dopant profile and cell parameters, for shallow (0.1 - 0.2 μm) junctions in single-crystal silicon. For cell preparation we have chosen phosphorus, which is the most commonly used dopant in junction processing.

2. EXPERIMENTAL

We have used 3" single-crystal Si(100) wafers from a single batch, supplied by Wacker Chemitronic. They were one-sided polished, p-type (boron doped) and all showed identical resistivity (specified 2-5 Ωcm). Before implantation 2×2 cm^2 samples were cut out of the wafers. The front side of these samples was implanted up to a dose of 3×10^{15} cm^{-2} with 10 keV P^+. The back side was implanted with 2×10^{15} cm^{-2} 20 keV B^+, in order to obtain a degenerate p^+ layer. The edges (0.5 mm) of the samples were covered to avoid implantation of the sides. After implantation, the samples were cleaned in HCl to remove possible contaminants.

Pulsed-laser annealing was performed using a Q-switched ruby laser with a pulse length of 20 ns and a maximum pulse energy of 3 Joule. In order to be able to define the energy density on the samples with the accuracy needed to obtain a shallow junction, the laser beam was homogenized using a guide diffuser (6). In this way it was possible to achieve a combined spatial and temporal accuracy of ± 7% over a circular area of 5 mm diameter. To anneal the 4 cm^2 samples, the diffuser was stepped over the surface in a triangular pattern, with 3 mm spot-to-spot distance. All annealings were performed in air, at room temperature. After p.l.a. of front and back, a 10 min. 450°C thermal anneal was applied to remove quenched-in defects (7,8). Sheet resistance of the samples was measured using a four point probe.

The cells were finished by applying evaporated Ti/Pd/Ag contacts on front and back, using mechanical masks. The grid coverage was 10%. After evaporation, the samples were sintered at 450°C to obtain Ohmic contacts. To avoid a spread in the short circuit currents, no anti-reflective coating was applied.

Dopant redistribution was determined using Rutherford Backscattering Spectrometry (RBS). Electrical characterization of the cells was performed under 1000 W/cm^2 AM1 irradiation, at 25°C. Using a recently developed curve fitting procedure (9), it was possible to determine all parameters in a two-diodes model to describe the electrical behaviour of the cells (see Fig. 1). In addition, spectral response measurements were done.

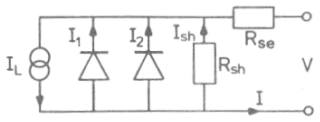

Fig. 1. Two-diodes representation of a p-n junction solar cell under illumination.

$$I = I_L - I_{01}(e^{eV'/kT} - 1) - I_{02}(e^{eV'/2kT} - 1) - V'/R_{sh}$$

$$V' = V + IR_{se}$$

3. RESULTS AND DISCUSSION

When preparing a shallow p-n junction using ion implantation, it is essential to choose the energy of the implanted species as low as possible. For many implanters the minimum voltage which yields a reasonable beam current, is about 10 kV. We have also chosen this value in our experiments. The projected range of 10 keV P^+ in silicon is 14 nm, while the region of amorphization extends to about 30 nm. Fig. 2 shows the sheet resistance (R_{sheet}) of the P-implanted layer as a function of pulsed-laser energy density. With increasing energy density, the melt depth increases and the implanted P atoms are spread so that the average dopant concentration decreases. Using p.l.a., complete electrical activation of dopant can already be obtained at low energy densities (10), therefore the gradual decrease in R_{sheet} with increasing energy density is attributed to a change in carrier mobility rather than to an increasing number of carriers.

The relation between the open-circuit voltage (V_{oc}) of the completed cells and the laser energy density used for the annealing of the emitter is given in Fig. 3 (the back-side implantation was activated by p.l.a. in the same way for all cells, at 1.3 J/cm^2). Fig. 3 shows that V_{oc} initially increases with increasing energy density and reaches a maximum at ≈ 1.3 J/cm^{-2}. At 1.9 J/cm^{-2} V_{oc} is lower, probably due to surface damage.

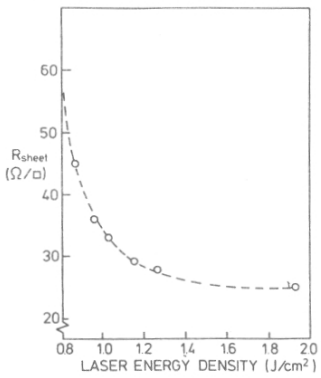

Fig. 2. Sheet resistance of phosphorus-implanted silicon (3×10^{15} cm^{-2} 10 keV P^+) as function of pulsed-laser energy density

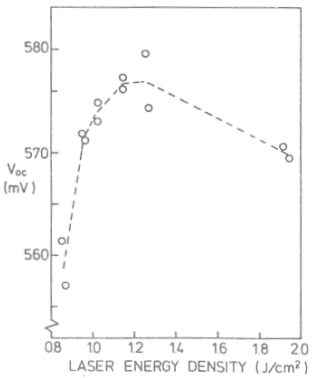

Fig. 3. Open-circuit voltage as function of pulsed-laser energy density.

Because of the small difference in mass between Si and P it is impossible to measure the concentration profiles of P in Si with RBS. However, from measurements of As profiles after p.l.a. of 10 keV As^+ implantations, we deduce that a laser energy density between 0.9 and 1.3 J/cm^2 corresponds to a melt depth between 0.1 and 0.2 μm. Note that this is almost an order of magnitude larger than the original amorphized layer thickness.

We have used a curve fitting procedure to determine all parameters in a two-diodes model to describe a p-n junction cell (see Fig. 1) (11,12). In

this model V_{oc} is mainly determined by the reverse saturation currents I_{01} and I_{02}. I_{01} originates mainly from neutral regions in the emitter and base of the cell, I_{02} from space-charge regions. In our case the junction depletion region is highly asymmetric and lies almost completely in the p-type base of the cell. It extends from the emitter (≈ 0.2 μm) to about 1 μm depth. Fig. 4 shows the reverse saturation currents I_{01} and I_{02} as a function of laser energy density. The sharp decrease in I_{01} between 0.85 and 0.95 J/cm² is related to improving the quality of the emitter with increasing melt depth. Apparently, 0.85 J/cm² is insufficient to obtain perfect epitaxy over the entire area of the cell. This can either be due to a high concentration of defects in the underlying (seed-) crystal, or to inhomogeneities in the energy density, which become very important when the energy is just above threshold for complete melting of the amorphized layer (0.7 - 0.8 J/cm²). Increasing the energy density from 0.95 J/cm² to 1.25 J/cm² hardly changes I_{01}, indicating that the crystal quality of the emitter is not improved further. At 1.9 J/cm², we observe some surface damage, which results in an increased I_{01} component. Fig. 4 also shows that the dark current component I_{02} decreases steadily with increasing energy density. As we attribute I_{02} mainly to defects within the depletion region, its behaviour as function of energy density suggests that melting beyond the original amorphous-crystalline interface reduces the concentration of electrically active defects in the depletion region. It has been reported (13,14) that the P implantation profile shows a tail, which extends far beyond the amorphized top layer. This tail has been explained by the occurrence of channeling of P ions into the single crystal substrate. Probably by increasing the melt depth, defects resulting from these channeled P ions are removed.

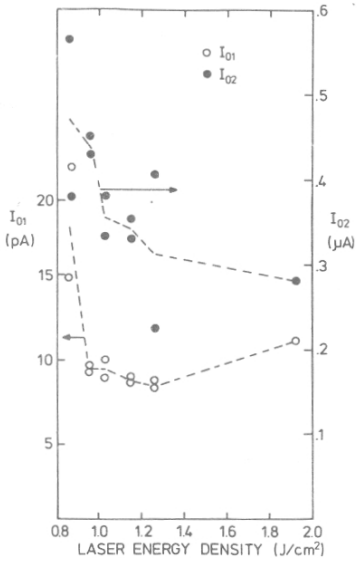

Fig. 4. Reverse saturation currents I_{01} and I_{02} as function of pulsed-laser energy density (see Fig. 1 and text).

Fig. 5 shows the short-circuit current (I_{sc}) as a function of laser energy density. Overall, I_{sc} decreases with increasing energy density, which must be due to the increasing thickness of the heavily doped emitter region with low quantum efficiency. This is further illustrated by Fig. 6 which shows the external quantum efficiency at λ = 453 nm, as a function of energy density. At this wavelength, the absorption depth of photons in (intrinsic) Si is about 0.5 μm so there is a strong relation between emitter thickness and quantum efficiency. Fig. 7 shows the external quantum effi-

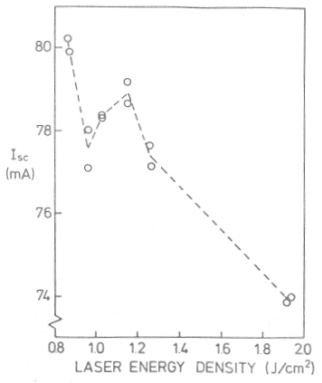

Fig. 5. Short-circuit current as function of pulsed-laser energy density.

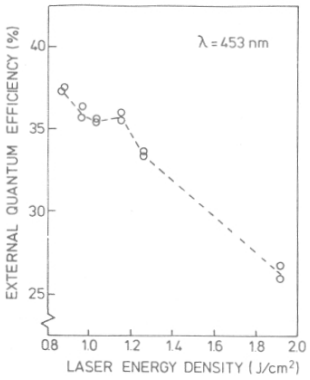

Fig. 6. External quantum efficiency at λ = 453 nm as function of pulsed-laser energy density.

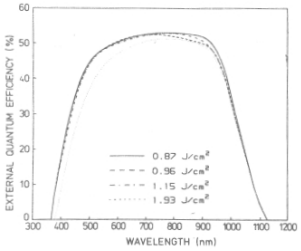

Fig. 7. External quantum efficiency as function of wavelength for various pulsed-laser energy densities.

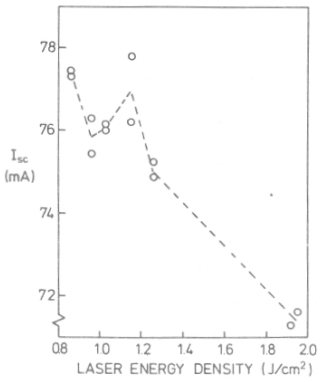

Fig. 8. Short-circuit current as function of pulsed-laser energy density, calculated from quantum efficiency measurements.

ciency as a function of wavelength for different laser energy densities. This figure indicates that in addition to the short wavelength absorption effect, the quantum efficiency for longer wavelengths is also affected when the laser energy density is increased from 0.85 J/cm^{-2} to 1.15 J/cm^{-2}. We suggest, that this results from changes in the reflection coefficient and is related to the carrier profile within the emitter.

We have used quantum efficiency measurements to calculate the short circuit current as a function of energy density (given the spectrum of the AM1 simulator). The results are given in Fig. 8. The behaviour of I_{sc} in this figure agrees very well with that of the measured I_{sc} values in Fig. 5.

4. CONCLUSIONS

Although we have used low-energy (10 keV) phosphorus implantation which yields an amorphous layer of only ≈ 0.03 μm, it requires an emitter thickness > 0.2 μm to obtain an optimal V_{oc} (577 mV). From analysis of the junction diode behaviour we conclude that the relatively low V_{oc} (≈ 560 mV) for thin emitters is due to incomplete removal of implantation-tail damage. In contrast to V_{oc}, I_{sc} decreases with increasing emitter thickness. This is related to an enhanced photon absorption in the low-lifetime n^+ region of the cell, so it would be desirable to reduce the emitter thickness to ≈ 0.1 μm. To obtain an optimum V_{oc} for a very shallow junction (≈ 0.1 μm), it is necessary to avoid channeling of implanted ions into the substrate. In addition we conclude that it is possible to determine all parameters in a two-diodes description of the cell characteristic from one I(V) curve measured under illumination.

5. ACKNOWLEDGEMENTS

The authors wish to thank S. Doorn for the ion implantation and G.P.A. Frijlink for the evaporation of contacts.

This work is part of the research program of the Stichting voor Fundamenteel Onderzoek der Materie and was financially supported by the Nederlandse Organisatie voor Zuiver Wetenschappelijk Onderzoek.

REFERENCES

(1) R.T. Young, R.F. Wood and W.H. Christie. J.Appl.Phys. 53, 1178 (1982).
(2) R.T. Young et al. IEEE Trans.Electron Devices ED-27, 807 (1982).
(3) D.H. Lowndes et al. Appl.Phys.Lett. 41, 938 (1982).
(4) G. Zoncini and F. Zignani. In Report nr. EUR 8215 EN, Commision of the European Communities (1984).
(5) J.S. Katzeff, M. Lopez and D.R. Burger. Proc.15th IEEE P.V. Spec.Conf., 437 (1981).
(6) A.G. Cullis, H.C. Webber and P. Bailey. J.Phys.E: Sci.Instrum. 12, 688 (1979).
(7) W. Sinke et al. Proc.5th E.C. P.V. Solar Energy Conf., ed. W. Palz and F. Fittipaldi, Reidel Publ., 1095 (1984).
(8) A. Mesli, J.C. Muller, D. Salles and P. Siffert. Appl.Phys.Lett. 39, 159 (1981).
(9) A. Polman, W.G.J.H.M. van Sark, W. Sinke and F.W. Saris. To be published.
(10) M. Miyao, K. Itoh, M. Tamura, H. Tamura and T. Tokuyama. J.Appl.Phys. 51, 4139 (1980).
(11) M. Wolf, G.T. Noel and R.J. Stirn. IEEE Trans.Electron Devices ED-24, 419 (1977)
(12) A.S. Grove. In Phys.and Technol.of Semicond.Devices, Wiley, N.York (1967).
(13) P. Blood, G. Dearnaley and M.A. Wilkins. Rad.Eff. 21, 245 (1974).
(14) G. Dearnaley et al. Can.J.Phys. 46, 587 (1968).